BBC
BROWN BOVERI

A NEW SOLID STATE LOSS OF EXCITATION RELAY FOR INTERTIE APPLICATIONS

CHRISTIAN A. BORNER STANLEY E. ZOCHOLL

BROWN BOVERI ELECTRIC
PROTECTIVE RELAY BUSINESS
HORSHAM, PA

PRESENTED BEFORE THE NINTH ANNUAL
WESTERN PROTECTIVE RELAY CONFERENCE
OCTOBER 26-28, 1982

Brown Boveri Electric

A NEW SOLID STATE LOSS OF EXCITATION RELAY FOR INTERTIE APPLICATIONS

ABSTRACT

This paper discusses the design of a new solid state self-compensating loss of excitation relay for synchronous machines. System conditions during loss of excitation of a machine are reviewed. The machine parameters and the impedance trajectory during the power swing are analyzed which lead to the characteristics used for loss of excitation protection.

INTRODUCTION

The subject of this paper is a new solid-state 50/60 hertz off-set mho relay for loss of excitation protection for generators. The relay complements the series of solid state protective relays designed for generator protection discussed by Waldron and Zocholl.[1] These relays share a common design goal of a rugged compact design fitting one standard case conserving valuable panel space and weight. At the same time these relays meet difficult environmental conditions and are suitable for nuclear Class 1E applications.

The subject relay was designed to meet these same goals and to provide a mho characteristic conveniently adjustable over a range sufficient for a wide range of generator applications. A particular goal was to provide this protection at cost feasible for small as well as large capacity generators.

LOSS OF EXCITATION PROBLEM

Loss of excitation can be caused by a fault in the generator field windings, a failure of the excitation source, or by operator error. In a critically loaded machine, the resulting drastic reduction in generator internal voltage causes a power swing and the ultimate loss of stability.

The loss of excitation problem may be analyzed using the two machine system of Figure 1. In Figure 1 the bus represents the terminals of generator A with an internal reactance X_d and voltage E_A. The reactance X_S is the system reactance viewed from the generator terminals and E_B is the internal voltage of the equivalent system generator B.

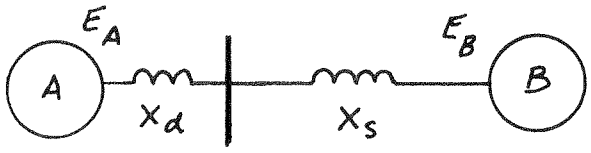

FIGURE 1. GENERATOR AND SYSTEM EQUIVALENT

Equations (1) and (2) describe the power output and dynamic behavior of generator A.

$$P_0 = \frac{E_A \, E_B}{X_d + X_s} \sin \delta \qquad (1)$$

$$P_1 - P_0 = M \frac{d^2 \delta}{dt^2} \qquad (2)$$

P_0 is the electrical output power of generator A and is a function of the two voltage magnitudes, the phase angle, δ, between the two voltages and the total system reactance.

In equation (2), P_1 is the mechanical input power and M is the inertia constant of the machine and its prime mover. Equation (2) is a form of the fundamental relation that torque equals moment of inertia times acceleration.[2] Accelerating torque is expressed as the difference of mechanical input and electrical output while acceleration is expressed as the change in voltage phase angle indicating a deviation from synchronous speed.

Normal synchronous operation is a state of equilibrium where the imbalance of power in equation (2) is zero and there is no departure from synchronous speed. With loss of excitation, power output P_0 falls with E_A and the imbalance of power expressed by equation (2) causes rotor acceleration. If the angle advances to the point of maximum power transfer without restoring the power equilibrium, stability will be lost.

Loss of excitation is detrimental to the system and the machine. The machine, normally a VAR source maintaining system voltage, becomes a VAR load when its voltage drops below system voltage. System voltage is depressed and the remaining machines must supply not only the system VAR deficit but also the generator VAR load.

The machine driven above synchronous speed, without field, and with its VAR loss supplied by the system constitutes an induction generator. The slip frequency between the stator field and the rotor induces current in the rotor in the manner of an induction machine. The current returning at the ends of the rotor quickly overheat end rings and wedges to the point of damage.

Consequently, loss of excitation protection is required for both system and machine considerations.

R-X PLANE

The characteristics of directional VAR and power factor relays map on to the R-X plane as whole quadrants or sectors which are encroached by power swings caused by system disturbances other than loss of excitation. The offset mho relay is used because its characteristic can be placed to enclose an area intruded only by power swings caused by loss of excitation where stability loss is inevitable.

In her paper analyzing the trajectories of power swings in the impedance plane and their effect on distance relays, Edith Clarke[3] traces the history of the graphical method using the R-X diagram to determine relay performance. J. H. Neher[4], in a paper on the performance of distance relays, plots the characteristic curves of the boundry operation of various types of relays in terms of resistance and reactance.

In his discussion of a paper by C. R. Mason[5] presented at the same AIEE Convention in 1937, Mr. Neher[6] points out that system impedance seen by relays during power swings can likewise be plotted on the same chart as the relay characteristics. The graphical method was applied to the loss of excitation problem by C. R. Mason in reference 7 and the essence of this work is shown in Figure 2.

In Figure 2, the origin of the R-X plane is the generator bus of the two machine system of Figure 1. The generator reactance X_d, back of the bus is plotted as the line OA on the negative reactance axis. The system reactance, X_S, in front of the bus is plotted as the line OB on the positive reactance axis. Half way between A and B is the point M, the electrical center of the system. The circle centered at M and passing through A and B is the stability limit for the system. The line AB may be viewed as the voltage difference between the internal voltages E_A and E_B and the lines drawn to the point N on the circle are the phasors E_A and E_B. This circle is the locus of all points where the angle between E_A and E_B is 90^o, the angle of maximum power transfer.

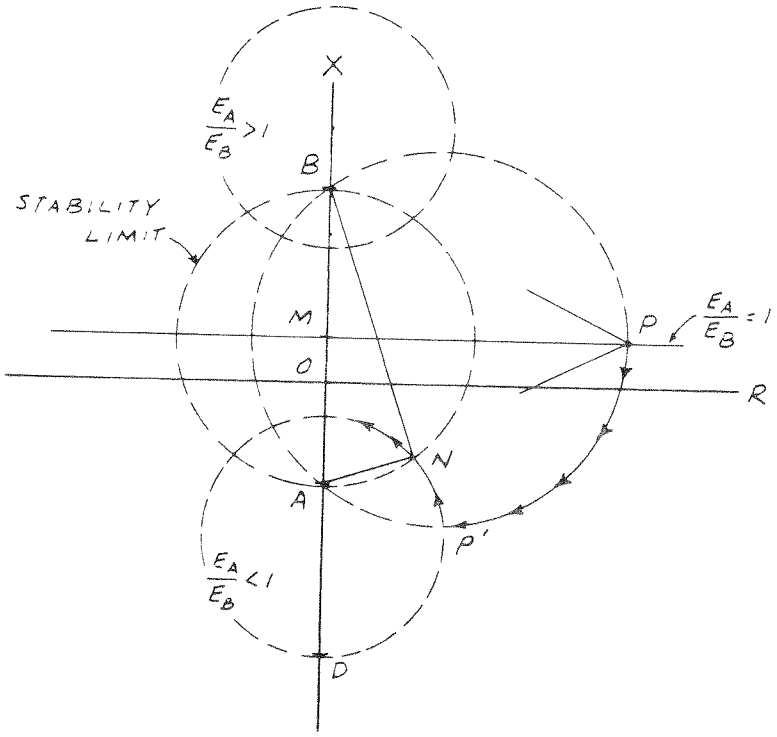

FIGURE 2. IMPEDANCE DURING SWINGS

CIRCLES OF CONSTANT ANGLE

Extend this observation to the circle, ABP, centered on the line MP to the right of the reactance axis. This circle is the locus of all points where the angle is constant but less than 90^{o}. Consequently, there exist an infinite number of such circles centered on the line MP on which the angle is constant and the angle increases as the center moves toward the left.

CIRCLES OF CONSTANT EXCITATION

The locus of points where the voltage ratio E_A/E_B is constant are also circles when mapped in the R-X plane with centers on the reactance axis. The line MP is significant in that it is the circle of infinite radius and locates all points where E_A equals E_B. Circles of constant ratio less than one have their center below the line MP on the reactance axis. The circle DPN is such a plot where E_A is one third of E_B. This observation can be checked by examining the phasors AN and BN which have that ratio. Also, an infinite number of these circles exist. Their centers move toward the point A with diameters converging into the point A as E_A/E_B goes to zero.

A similar set of circles exist for E_A/E_B greater than one. Their centers are on the reactance axis above the line MP and converge into the point B as the ratio goes to infinity. These circles describe the condition for loss of excitation in generator B while the circles below the line MP describe the loss of excitation states for generator A.

POWER SWING IMPEDANCE

The probable path of the power swing caused by the loss of excitation can be determined by using the constant ratio and angle circle diagrams of Figure 2. For example, an initial operating point P is chosen where the voltage magnitudes are equal and the angle between them is approximately 50^{o}. If the magnitude of E_A, by loss of field, could be lowered to one third of its value before inertia would allow angular change, the operating point would move along the constant angle circle ABP to point P'.

The power difference created by the fall in voltage then causes rotor acceleration and movement of angle along constant voltage circle in the direction of increasing angle. This is the path P' at 50^{o} toward point N where the angle is 90^{o} and beyond to 180^{o} where the generator slips a pole.

In the actual case, the decay of voltage due to complete loss of the excitation source is gradual, taking place in a period of seconds. Tramaine and Blackburn[8] report asynchronous operation as long as six seconds before the out of step condition takes place. Consequently, the decay of voltage and angular change occur concurrently.

DIAMETER OF THE MHO CHARACTERISTIC

The trajectory developed in Figure 2 indicates that the mho characteristic should be placed on the reactance axis and enclose the final value of reactance

on the 180^{o} axis. The path shows this to be a point in the generator reactance 0A.

However, the generator reactance is variable, its value depending on whether the slip frequency of the swing is high enough to induce current in the transient paths of the machine. Thus, the reactance can vary between direct axis, transient reactance X'_d, and direct axis synchronous reactance X_d. Higher slip frequencies are associated with fully loaded machines since there is more mechanical input power for acceleration.

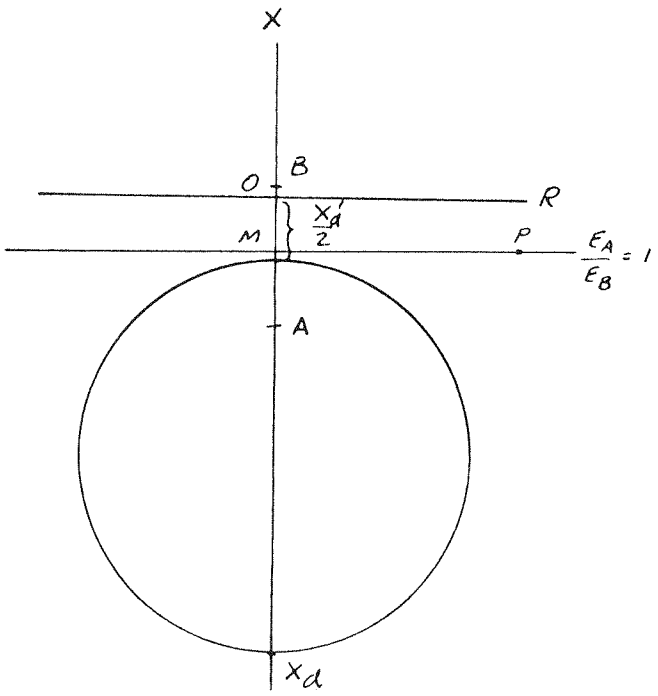

FIGURE 3. OFF-SET MHO CHARACTERISTIC AND EQUAL VOLTAGE LOCUS

OFF-SET OF THE MHO CHARACTERISTIC

The off-set of the mho characteristic is determined by system reactance. The limiting case is that of a small generator feeding an infinite bus. In this case, the system reactance is virtually zero and the line of equal voltage MP bisects the generator reactance as shown in Figure 3. Thus, the off-set should be half the minimum generator reactance or $\frac{X_d'}{2}$.

The mho characteristic with off-set gives the greatest selectivity and security being unaffected by power swings and faults in the system.

PRINCIPLE OF OPERATION

As shown above, the relay should trip if the impedance vector seen from the generator falls into a circle below the real axis of the impedance plane. This circle is defined by the two vectors $-jX_1$ and $-jX_2$. (See Figure 4.)

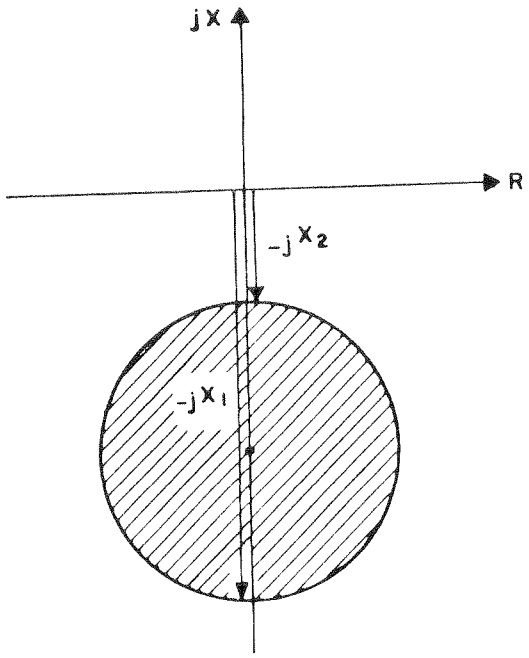

FIGURE 4. RELAY CHARACTERISTIC

To determine if the impedance vector falls into the circle or not, first the following two differences are developed:

$$D_1 = V - (-jX_1)I \tag{3}$$

$$D_2 = V - (-jX_2)I \tag{4}$$

Equations (3) and (4) can be simplified to:

$$D_1 = V + jX_1I \tag{5}$$

$$\text{and } D_2 = V + jX_2I \tag{6}$$

According to Figure 5, the relay should trip if the phase angle between D_1 and D_2 is greater than or equal to 90^0.

Figure 6a shows the principle of a relay with the desired characteristic. For this figure we let

$$k_1 = jX_1 \tag{7}$$

$$\text{and } k_2 = jX_2 \tag{8}$$

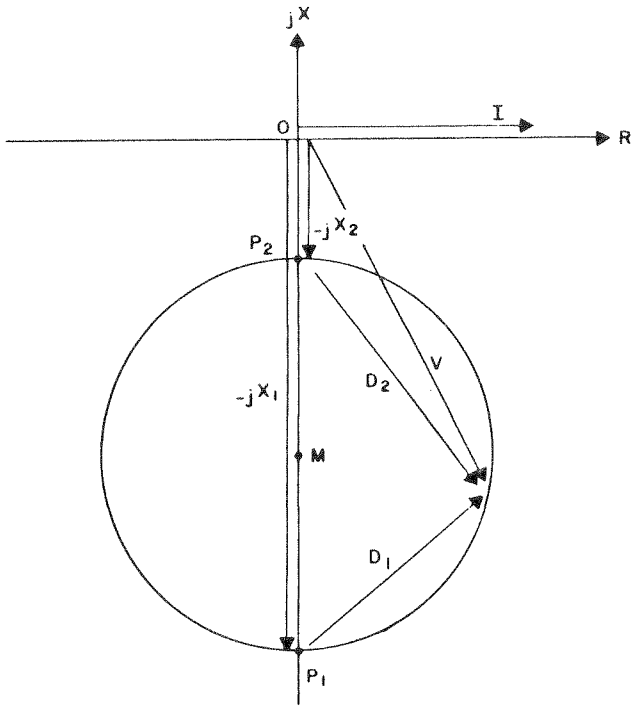

FIGURE 5. DIAGRAM SHOWING THE PRINCIPLE OF OPERATION

After the summing junctions, the signals D_1 and D_2 can be shaped because the phase remains the same in the sine wave and square wave.

Since the operator j denotes a 90^o phase shift and further some filtering of the input signal is needed, Figure 6a can be changed to Figure 6b. The filters F_1 and F_2 have a transfer function of g_1 and g_2 respectively. For the relay only the difference of the phase shift in the two filter circuits is of importance. We let the difference of the phase shift be 90^o at the operating frequency. In addition we let $|g_1| = 1$ and $|g_2| = 1$ at this frequency. Considering the conversion of the input current to a voltage V_R by resistor R and the above, we get for the absolute values of k_1 and k_2:

$$|k_1| = k_1' \cdot R \tag{9}$$

$$\text{and } |k_2| = k_2' \cdot R \tag{10}$$

Substituting for k_1 and k_2 and expressed in terms of k_1' and k_2' respectively, equations (9) and (10) are as follows:

$$k_1' = \frac{X_1}{R} \tag{11}$$

$$k_2' = \frac{X_2}{R} \tag{12}$$

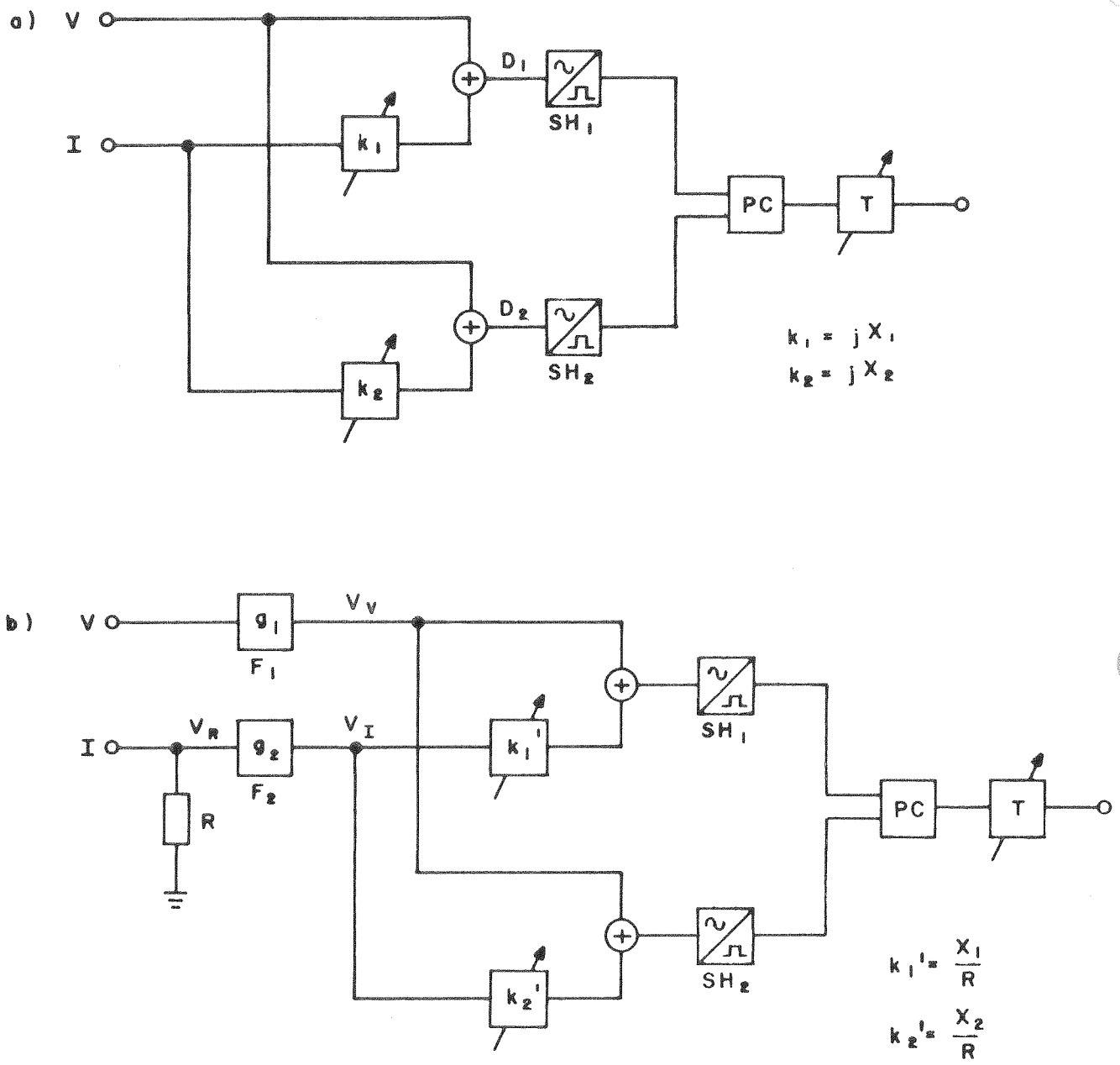

FIGURE 6. BLOCK DIAGRAMS OF THE RELAY

DESIGN OF THE INPUT CIRCUITS

It is obvious that the difference of the phase shift of the two input filters not only should be 90° at the operating frequency but also should be close to 90° over a wide frequency range. In addition, the relay should operate from 60 Hz as well as from 50 Hz with only minor changes.

Two similar two-pole low pass circuits were chosen as input filters for the two signal inputs. It can be seen from Figure 5 that $|D_1|$ becomes zero if V is equal to OP_1. Substituting in equation (5) this can be expressed as

$$\frac{V}{I} = -jX_1 \qquad (13)$$

Referring to Figure 6b, with the transfer functions g_1 and g_2 for the filters F_1 and F_2 respectively, this can also be written as:

$$V \cdot g_1 = -I \cdot R \cdot g_2 \cdot k_1' \qquad (14)$$

$$\frac{V}{I} = -\frac{R\, g_2\, k_1'}{g_1} \qquad (15)$$

Substituting equation (13) into (15) we get

$$\frac{R \cdot g_2 \cdot k_1'}{g_1} = jX_1 \qquad (16)$$

The phase shift of 90° denoted by j in equation (16) also means that the real part is equal to zero. Since we want an exact 90° shift at 50 Hz and 60 Hz we let

$$\mathrm{Re}\left[\frac{g_2}{g_1}\right] = 0 \qquad (@\ 50\ \mathrm{Hz\ and\ 60\ Hz}) \qquad (17)$$

at these two frequencies. Note that the scaling factors are not needed.

For the design we first chose the characteristic of the first filter, (e.g. the coefficients) and then we calculated the coefficients of the second filter by using equation (17).

With this design the difference of the phase shift of the two filters is close to 90° over a broad frequency range (see Figure 7 and Table 1).

Although the 90° difference between the filters F_1 and F_2 also easily could be achieved with F_2 having only one pole, a two pole filter was chosen with the second cut off frequency well above 60 Hz. With this two pole filter, we achieve a superior suppression of the harmonics. This suppression is in contrast to the current to voltage transducers of other relays which amplify the harmonics.

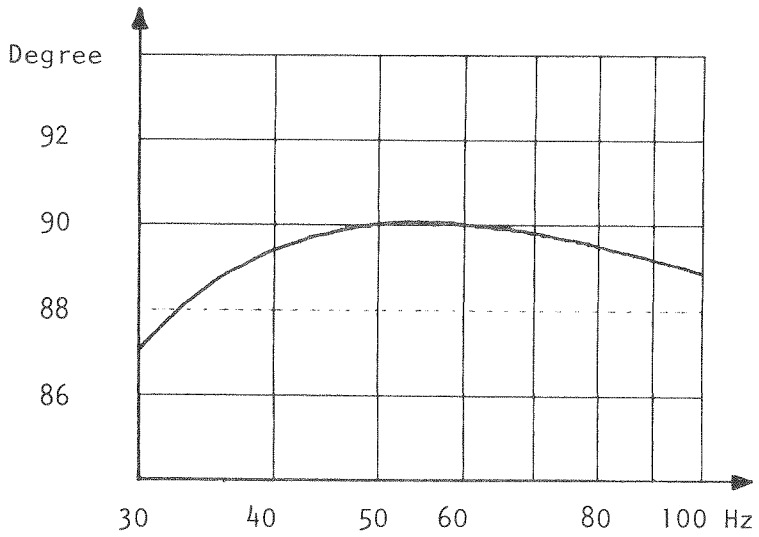

FIGURE 7. PHASE SHIFT VERSUS FREQUENCY

REPRESENTATION OF THE GENERATOR REACTANCE

The relay is set according to the reactance of the generator. Since this reactance changes proportionally to the frequency, the tripping points also should change proportional to the frequency. Because the voltage is filtered by F_1, a two-pole filter, the output voltage V_V is essentially proportional to V/f^2. Similar in the current path with F_2, the voltage developed across R is filtered. But because the second cutoff frequency is well above 60 Hz, the resulting voltage V_I is proportional to $1/f$ in the considered range.

Therefore we can say:

$$\frac{V_V}{V_I} \simeq \frac{V/f^2}{I/f} = \text{constant} \qquad (18)$$

or from (18):

$$\frac{V}{I} \sim f \qquad (19)$$

Figure 8 and Table 1 show how the tripping reactances change.

Since the considered frequency range is near the cutoff frequencies, equation (19) is an approximation. Table 1 and Figure 9 show the error of the amplitudes of the tripping reactances which is calculated as follows:

$$\Delta X = \frac{g_2\, f}{g_1\, f_o} - 1 \qquad (20)$$

where f_o is 50 Hz and 60 Hz respectively.

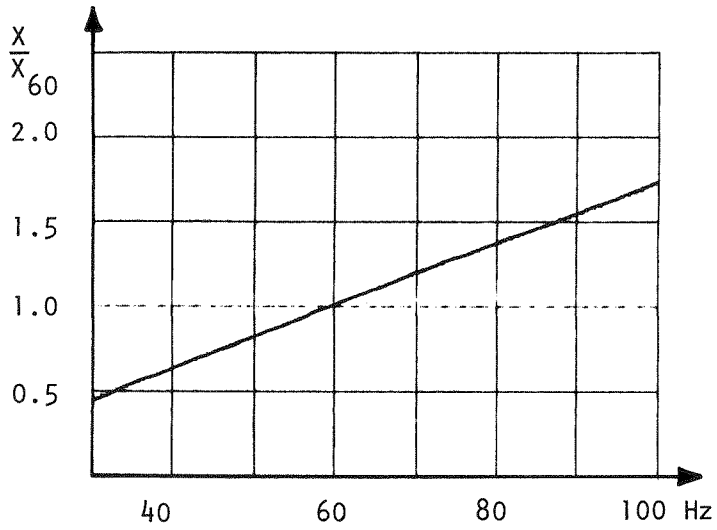

FIGURE 8. NORMALIZED IMPEDANCE VERSUS FREQUENCY

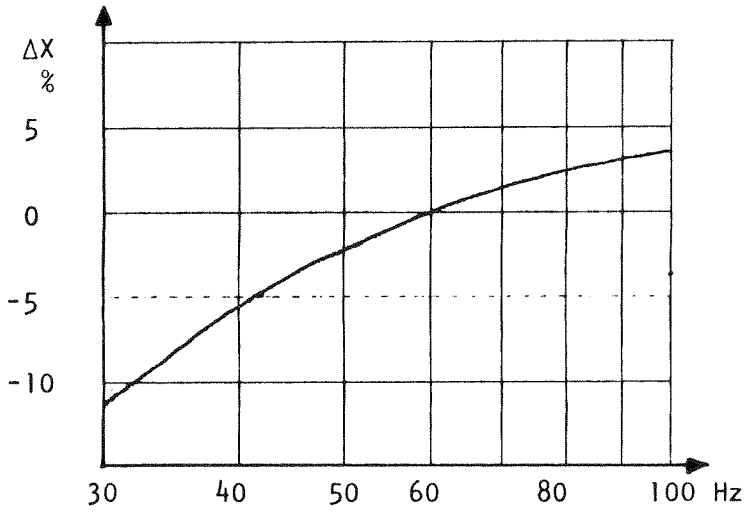

FIGURE 9. IMPEDANCE ERROR VERSUS FREQUENCY

NOMINAL FREQUENCY	% CHANGE OF FREQUENCY	ERROR OF PHASE SHIFT (DEGREE)	NORMALIZED TRIPPING REACTANCE	ERROR OF AMPLITUDE (%)
60 Hz	20	-0.26	1.220	1.65
	10	-0.11	1.110	0.93
	5	-0.05	1.055	0.49
	2	-0.02	1.022	0.20
	0	0.00	1.000	0.00
	-2	0.02	.978	-0.21
	-5	0.03	.945	-0.56
	-10	0.04	.889	-1.20
	-20	-0.05	.778	-2.77
50 Hz	20	0.00	1.227	2.24
	10	0.04	1.114	1.25
	5	0.03	1.057	0.66
	2	0.02	1.023	0.27
	0	0.00	1.000	0.00
	-2	-0.02	0.977	-0.29
	-5	-0.07	0.943	-0.74
	-10	-0.18	0.886	-1.58
	-20	-0.59	0.771	-3.59

TABLE 1

SETTING OF THE RELAY

Most of the known loss of excitation relays are set with taps on the voltage transformer, therefore, the resulting setting on ohms is inverse to the tap setting. The tap setting must first be calculated before the settings can be done.

In contrast to this setting procedure, the settings in the new relay are done in the current path. As you can see from Figure 6b, k_1' and k_2' can be varied. With convenient thumbwheel switches, k_2' can be set from 10 to 159 ohms in 1.0 ohm steps. Similar k_2' can be set for an offset (X_2) of 0 to 7.5 ohms in .5 ohm steps. The time delay of this relay is also set by thumbwheel switches from .2 to 3.0 seconds.

CONCLUSIONS

The phasor difference and phase comparison functions necessary for the offset mho characteristic are ideally implemented with solid state circuitry. These circuits provide for linear rather than inverse setting controls which allow accurate calibration over a wide range of adjustment. Input filters surpress unwanted harmonics and also maintain the required quadrature phase shift between the input voltage and current over the range of frequency experienced during the loss of excitation power swing.

These features allow a compact, rugged, and cost effective design suitable for generators with a wide range of settings.

REFERENCES

1. S. E. Zocholl, J. E. Waldron, "Solid State Relays for Generator Protection", Sixth Annual Western Protective Relay Conference, Oct. 1979.

2. W. D. Stevenson, Jr., "Elements of Power System Analysis", McGraw-Hill Book Co., 1955, 325-330.

3. Edith Clarke, "Impedance Seen by Relays During Power Swings With and Without Faults", AIEE Transactions, Vol. 64, 1945, pp 372-84.

4. J. H. Neher, "A Comprehensive Method of Determining Performance of Distance Relays", AIEE Transactions, Vol. 56, 1937, pp 833-44.

5. C. R. Mason, "Relay Operation During System Oscillations", AIEE Transactions, Vol. 56, 1937, pp 823-32.

6. Discussion by J. H. Neher of Reference 4, AIEE Transactions, Vol. 56, 1937.

   Closure by C. R. Mason of Reference 5, AIEE Transactions, Vol. 57, 1938, pp 111-14.

7. C. R. Mason, "A New Loss of Excitation Relay for Synchronous Generators", AIEE Transactions, Vol. 68, Pt. II, 1949, pp 1240-1245.

8. R. L. Tramaine, J. L. Blackburn, "Loss of Field Protection for Synchronous Machines", AIEE Transactions, Vol. 73, Pt. III-A, 1954, pp 765-77.